Erschienen in: CrystEngComm ; 24 (2022), 26. - S. 4631-4832
https://dx.doi.org/10.1039/D2CE00511E

Synthesis of two-dimensional layered double hydroxides: a systematic overview

Zongkun Chen,[a] Qiqi Fan,[a] Minghua Huang *[b] and Helmut Cölfen *[a]

Two-dimensional (2D) layered double hydroxides (LDH) are classic materials in fundamental research and practical application. 2D LDH have unique structural features, such as high aspect ratio, high specific surface area, quantum confinement in one direction, layered structure, tunable intercalated anions/interlayer spacing/metal-cation compositions, *etc.*, which endow 2D LDH with excellent chemical and physical properties. Since rational production is the first and crucial step towards their utilization, numerous efforts have been devoted to explore innovative and effective methods for their preparation. This review is a comprehensive overview of synthesis methods and aimed to capture the features of different synthesis methods to enable the selection of a suitable method to achieve the desired LDH characteristics. Therefore, we systematically summarized various preparation methods of 2D LDH, including a top-down approach, bottom-up approach, and decomposition-regrowth strategy. Besides, we listed and compared the important parameters relating to both the synthesis process and the obtained products of various synthesis methods, such as the synthesis temperature/pressure, the used device, the utilized reactants, the presence or absence of pre/post-treatment, the yield, the crystallinity and the lateral size and thickness. Finally, some current challenges and further tasks regarding the synthesis of LDH are presented.

1. Introduction

Layered double hydroxides (LDH) are a large family of two-dimensional materials consisting of positively charged brucite-like host layers, as well as anions and solvent molecules in the interlayer space.[1,2] The general formula of LDH is $[M_{1-x}^{2+}M_x^{3+}(OH)_2]^{x+}[A_{x/n}^{n-}]^{x-}\cdot mH_2O$ (Fig. 1),[3–5] in which M^{2+} and M^{3+} are metallic divalent and trivalent cations, respectively, and A^{n-} are the interlayered anions.[6] Note that although most LDHs are binary, preparing ternary LDH, quaternary LDH and LDH containing more combinations of metals species is also possible.[7] The existence of interlayer anions could compensate for the positive charges that are produced by partial replacement of M^{2+} by M^{3+} in brucite-like host layers.[8] Due to the easy preparation, flexible structural composition, tunable interlayer space, exchangeable anions and unique physicochemical properties,[1,9,10] LDH have been regarded as attractive materials for a wide range of applications, such as catalysis,[9,11–24] energy storage,[25–31] drug delivery,[32,33] sensors,[34–37] flame retardants,[38] corrosion protection,[39–43] removing pollutants from natural environments,[44–47] preclinical/clinical nanomedicine,[32,33,48] bioimaging,[49] optoelectronic devices,[50] light-emitting applications,[1,51] photodetectors,[52] surface-enhanced Raman scattering,[53] polymer additives,[54] protein separation,[55] ultrafast separation of oil/water mixtures,[56] *etc.* Since the rational production of LDH is the first and crucial step towards their utilization, considerable research has been conducted over the past decade to explore their synthesis methods.[1,6,57–59] Considering that one in-depth review can serve as a reference guide for researchers in the area and help quickly capturing the advances of LDH in one place, there have been many reviews summarizing the progress on the synthesis methods of LDH.[60] For example, Chen *et al.*[60] summarized the recent progress on the development of exfoliation strategies for LDH including liquid phase

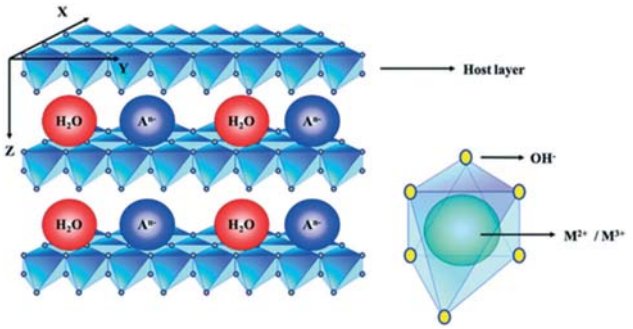

Fig. 1 The typical structure of LDH. Reproduced with permission from ref. 5.

[a] *Physical Chemistry, University of Konstanz, Universitätsstraße 10, D-78457 Konstanz, Germany. E-mail: helmut.coelfen@uni-konstanz.de*
[b] *School of Materials Science and Engineering, Ocean University of China, Qingdao 266100, China. E-mail: huangminghua@ouc.edu.cn*

exfoliation, plasma-induced exfoliation, and other advanced exfoliation strategies. Yang *et al.*[6] provided a comprehensive review on the development and progress in the synthesis of pristine LDH and modified LDH catalysts for advanced oxidation processes. Lu *et al.*[61] reviewed recent progresses on rational design of LDH nanosheets, including direct synthesis *via* traditional coprecipitation, homogeneous precipitation, and newly developed topochemical oxidation as well as chemical exfoliation of parent LDH crystals. However, a systematic introduction to the developed synthesis methods, their comprehensive comparison as well as a discussion of current challenges and further tasks regarding the synthesis of LDH are yet missing.

In this review, we systematically reviewed almost all already developed synthesis routes, and at least one example is discussed for each synthesis route, offering a comprehensive overview of the possible synthesis routes. Besides, we listed and compared several important parameters relating to both the synthesis process and the obtained products of these synthesis routes with a summary table, including the synthesis temperature/pressure, the used device, the utilized reactants, the presence or absence of pre/post-treatment, the yield, the crystallinity and the lateral size and thickness. We hope this table can act as a platform that can help researchers to easily understand the advantages and disadvantages of the existing synthesis routes, which is beneficial for selecting a suitable synthesis method according to the desired characteristics of the synthesis process and the obtained products. Furthermore, we also present some current challenges and further tasks regarding the synthesis of LDH, which is beneficial for helping us know how to facilitate the further development and effective utilization of LDH in daily life. It is expected that this review can provide fundamental insight into the synthesis of LDH for researchers and draw more attention to solve the tough problems that are impeding the further development of LDH. Note that, in this review, we focus on two-dimensional (2D) LDH based on the following considerations. First, compared to their bulk counterparts, 2D LDH possess unusual structural features, including high aspect ratio, high specific surface areas and quantum confinement in one direction, which can enable 2D LDH with unique electronic, optical, catalytic, mechanical and other properties.[1,9] Second, because LDH have the typical layered structure with weak van der Waals forces between (001) planes and strong in-plane chemical binding, LDH tend to preferentially grow along (001) planes to form 2D morphology during the growth process, which can be reflected by the fact that most of the LDH reported in previous studies present 2D morphology.[5,62]

2. Synthesis routes of 2D LDH

2D LDH are available as naturally occurring minerals and synthetic materials. The first synthesis of 2D LDH in the laboratory was realized by Feitknecht *via* the co-precipitation route in 1942.[63] Since then, various synthesis methods have been proposed and utilized to produce 2D LDH to meet academic and industrial demands. Although different synthesis methods have their features, they can be classified into three categories: top-down approach, bottom-up approach and decomposition-regrowth strategy.

2.1 Top-down approach

The top-down approach can realize the preparation of ultrathin 2D LDH nanosheets *via* decreasing the size of bulk (or micro) LDH. To be specific, this approach requires selecting an appropriate way to enlarge the interlayer distance and weaken the interlayer forces. According to the factors involved in the synthesis process, the preparation methods belonging to this approach can be divided into liquid phase exfoliation with pre-treatment, direct liquid phase exfoliation, and solid phase exfoliation. Liquid phase exfoliation is a process in which ultrathin nanosheets can be peeled off from the bulk LDH in the liquid media *via* overcoming the van der Waals force between layers, and solid state exfoliation is a strategy carried out on the LDH powders, instead of LDH dispersed in the liquid media.

2.1.1 Liquid phase exfoliation with pre-treatment. It is well known that the direct exfoliation for most LDH is quite difficult owing to the strong interactions between the host layers and anions, so that liquid phase exfoliation with pre-treatment, *i.e.* replacing original anions by other desirable organic/inorganic molecules or anions, was developed. Such strategy is regarded as one effective solution for addressing the above-mentioned problem, because, as shown in Fig. 2, it provides one possible way to enlarge the brucite interlayer distance and weaken the brucite interlayer forces.[64] In 1999, Adachi-Pagano *et al.*[65] realized the first complete exfoliation of LDH using such strategy *via* intercalating dodecyl sulfate (DDS) into $Zn_2Al(OH)_6Cl{\cdot}2H_2O$ in deionized water to obtain the expanded phase $Zn_2Al(OH)_6(C_{12}H_{25}SO_4){\cdot}nH_2O$ (ZnAl-DDS) with an increase of the basal spacing from 0.77 to 2.52 nm. Then, the complete exfoliation of ZnAl-DDS was realized by carrying out reflux in butanol at 120 °C for 16 h. It was proposed that the replacement of the interlayer water molecules by the solvent molecules might be the key process for the exfoliation. Besides, the authors found that water, methanol, ethanol, propanol, or hexane are no suitable solvents for exfoliating ZnAl-DDS, based on the fact that

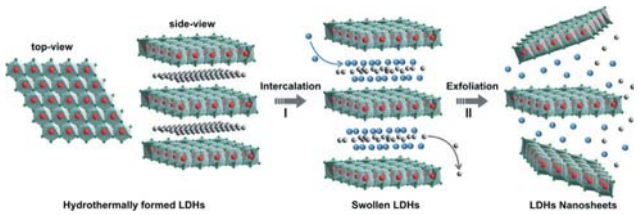

Fig. 2 Schematic illustration of the exfoliation process of LDH *via* liquid phase exfoliation with additional intercalation molecules or anions. Reproduced with permission from ref. 64.

conducting similar operations in these solvents leads to unstable suspensions that settled after a few hours and only a minor part of the material was dispersed. Later on, Singh *et al.* reported that the exfoliation of the unique LiAl-LDH depends on the structure of the intercalating surfactant in terms of both chain length and head group moiety, and LiAl-DDS-LDH cannot be successfully exfoliated in butanol,[66] suggesting that not all DDS intercalated LDH can be successfully exfoliated in butanol. Note that other solvents can be utilized to exfoliate bulk LDH into ultrathin nanosheets as well. For example, Naik *et al.*[67] achieved rapid exfoliation of LDH *via* stirring a pre-determined amount of DS^- intercalated MgAl-LDH and CoAl-LDH in toluene followed by sonication for 5 min (Fig. 4). The presence of the Tyndall effect indicates the formation of a colloidal suspension. Zhang *et al.*[68] reported a new strategy to exfoliate LDH by using supercritical ethanol. The procedure involves the intercalation of anionic surfactant into the decarbonated LDH by ion exchange, followed by an exfoliation of the surfactant-intercalated LDH in supercritical ethanol.

Except for DDS, other intercalation molecules or anions, such as NO_3^-,[69] graphdiyne,[70] laurate,[71] *etc.* can also be applied to exchange the original anions of LDH. Li *et al.* demonstrated the exfoliation of large MgAl-LDH crystals *via* shaking these bulk materials in formamide at room temperature.[72] Note that a pre-treatment, which involves treating MgAl–CO_3^{2-}-LDH in an aqueous solution containing appropriate amounts of $NaNO_3$ and HNO_3, is necessary for the successful exfoliation, because the tight association between CO_3^{2-} and the host layers increases the difficulty of exfoliation[69] and exchanging CO_3^{2-} by NO_3^- could weaken such interaction. In 2018, as shown in Fig. 3, Hui *et al.* described the *in situ* exfoliation and modification of bulk FeCo-LDH nanosheets through a graphdiyne-induced intercalation/exfoliation/decoration strategy, which allowed to exfoliate thick bulk LDH into ultrathin LDH nanosheets.[70]

In principle, ultrathin morphology of all LDH can be produced through liquid phase exfoliation with pre-treatment, because of their layered structure, that is hold together by van der Waals forces in one dimension. However, this strategy suffers from the following disadvantages: low

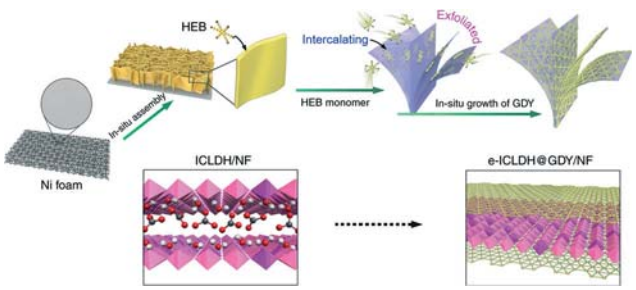

Fig. 3 Schematic representation of *in situ* exfoliation of bulk FeCo LDH nanosheets through a graphdiyne-induced intercalation/exfoliation/decoration strategy. Reproduced with permission from ref. 70.

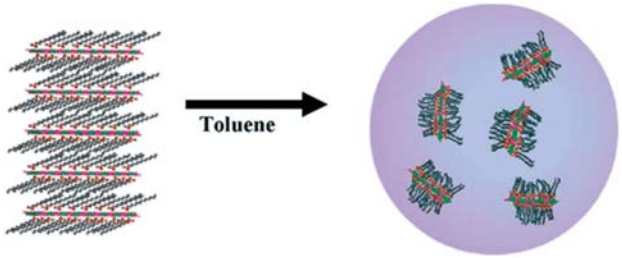

Fig. 4 Delamination of a surfactant-intercalated LDH in toluene. Reproduced with permission from ref. 67.

exfoliation efficiency, uncontrollability of the layer number/lateral size, the involvement of organic solvent and the possible contamination caused by organic molecule adsorption.

2.1.2 Direct liquid phase exfoliation. Since direct liquid phase exfoliation can realize the exfoliation of bulk LDH in liquid media without additional pre-treatment *via* replacing original anions with other molecules or anions, choosing an appropriate solvent is crucial for enlarging the brucite interlayer distance and weakening the brucite interlayer forces. Formamide has been regarded as an efficient solvent for the exfoliation of LDH, which can be reflected in the numerous studies that utilized formamide as a solvent. To be specific, in 2001, Hibino and Jones reported an approach to exfoliate LDH containing amino acid anions and glycine, which used formamide as the dispersant to create a desirable interlayer environment *via* uptaking a large amount of solvent.[73] Later, they reported that LDH containing amino acids could be exfoliated in formamide and a high amino acid content led to the failure of exfoliation due to the formation of a tight hydrogen-bonding network between amino acids and metal layers.[74] Gunjakar *et al.* demonstrated that ZnCr-LDH material can be exfoliated into individual monolayers *via* the dispersion of powdery LDH samples in formamide. The observation of a clear Tyndall effect indicates the formation of a colloidal suspension and that this suspension of the ZnCr-LDH ultrathin nanosheets is stable at room temperature for several weeks.[75] Park *et al.* decreased the thickness of bulk NiFe-LDH (100 nm) to 1 nm *via* exfoliating a precursor in argon purged formamide under vigorous stirring for 2 days.[76] Quan *et al.*[77] presented the exfoliation of NiMn-LDH in a formamide–water binary solution at 70 °C with continuous magnetic stirring for 8–24 h (Fig. 5). Note that, since formamide is a harmful and hardly eliminated solvent, much effort has been directed toward exploring other alternative solvents that can be employed in this strategy. For instance, Carrasco *et al.* investigated the influence of solvent on the exfoliation performance of LDH using a tip sonication methodology.[78] They found that *N*-cyclogexyl-2-pyrrolidon is the most suitable solvent for the direct exfoliation of CO_3^{2-}-LDH. Jobbágy *et al.*[79] treated $Mg_{0.71}/Al_{0.29}$-DDS^--LDH (DDS = dodecyl sulfate) in CCl_4 through a 30 min ultrasonication at room temperature, and

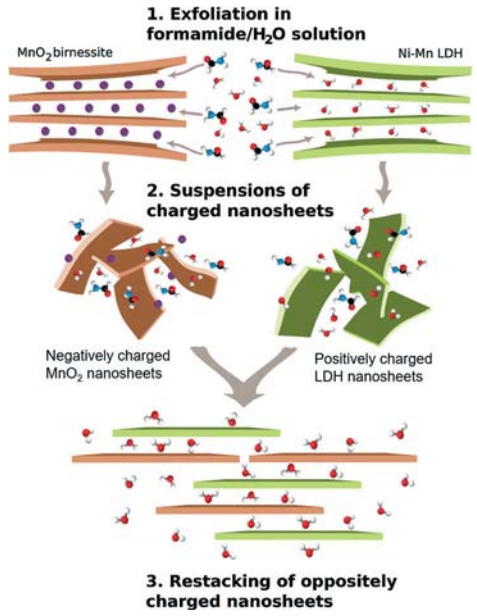

Fig. 5 General scheme for the preparation of the NiMn-LDH/MnO_2 composite obtained by restacking of oppositely charged nanosheets obtained by exfoliation of NiMn-LDH and MnO_2 in formamide/water solutions. Reproduced with permission from ref. 77.

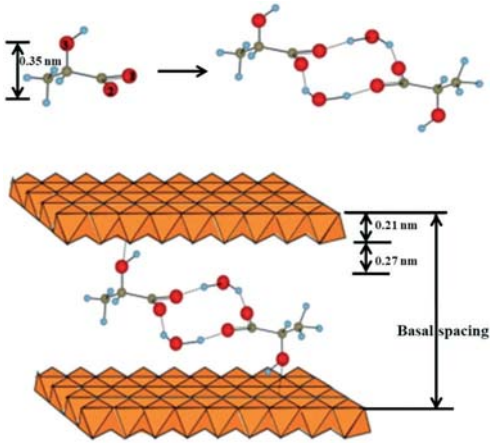

Fig. 7 Possible orientation of lactate anions in CoFeLc gallery. Reproduced with permission from ref. 81.

they found that the exfoliation can be successfully realized. As presented in Fig. 6, the authors proposed that CCl_4 molecules can solvate the hydrophobic tails of the intercalated anions (DDS^-), leading to the exfoliation of LDH. Antonyraj *et al.*[80] reported the one-step synthesis of CO_3^{2-}-free nitrate-containing LDH using a hexamethylenetetramine (HMT) hydrolysis method at low temperature. Meanwhile, they confirmed that the formed NO_3^--LDH could be successfully partly exfoliated in water and completely exfoliated in formamide. Atomic force microscopy (AFM) images show similar sheet thickness dimensions ranging from 2–10 nm both in formamide and water. As presented in Fig. 7, Zhu *et al.* proved that the insertion of lactate anions into MgAl or ZnAl-LDH made the exfoliation easy to be conducted in water.[81] Very recently, Munonde *et al.*[82] exploited the ultrasonic exfoliation of NiFe-LDH with the assistance of urea in water without any additional conditions. They proposed that the ultrasonic process can exfoliate the bulk NiFe-LDH into mono- and few-layer nanosheets because the stacked layers are exposed to an acoustic cavitation process, in which bubbles are created and collapsed in a solvent under ultrasound with a supply of high energy. This approach is regarded as one significant breakthrough in the field of exfoliating LDH due to the shorter treatment time and utilization of water as a solvent.

Note that external force is one important factor that can facilitate the successful exfoliation of bulk LDH *via* liquid phase exfoliation with pre-treatment or direct liquid phase exfoliation, and stirring, ultrasonication, low temperature, electrostatic repulsion, *etc.*, are commonly employed ways. For example, Li *et al.*[72] vigorously agitated a mixture (100 mL of formamide containing 0.05 g NO_3^--LDH) by a mechanical

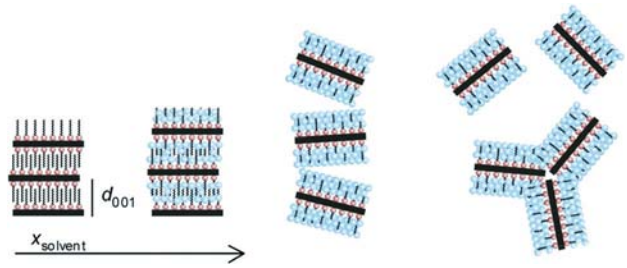

Fig. 6 Schematic representation of exfoliating $Mg_{0.71}/Al_{0.29}$-DS^--LDH in CCl_4. Reproduced with permission from ref. 79.

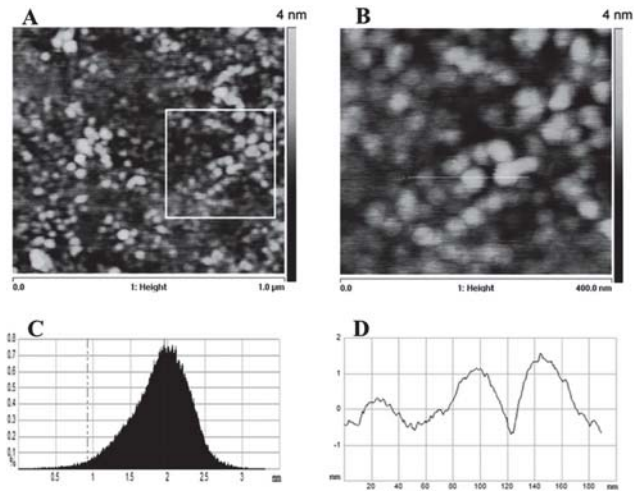

Fig. 8 AFM images of exfoliated NO_3^--LDH in formamide (0.1 g L^{-1}) deposited on a mica substrate. (A) Height image over a scanning area of 1000 × 1000 nm^2; (B) height image of the same sample over the marked scanning area of 400 × 400 nm^2; (C) depth histogram showing a maximum at 2 nm over the marked area; (D) section profile along the marked white line, showing single and double layers of exfoliated LDH. Reproduced with permission from ref. 83.

shaker at a speed of 170 rpm for 12 h, resulting in the formation of single-layer LDH nanosheets. Besides, Wu *et al.*[83] realized the exfoliation of MgAl–NO_3^--LDH in formamide by ultrasonication in successive intervals of 30 min until the turbidity of the solution became constant. Representative AFM images of delaminated NO_3^--LDH shown in Fig. 8 indicate that the nanosheets have an average thickness of 2 nm. Hou *et al.* reported that NiFe-LDH containing aminoundecanoic acid can be successfully exfoliated into LDH nanosheets by an electrostatic repulsive mechanism between the guest species and the inorganic host layers.[84] Wei *et al.* provided a simple but efficient method for the exfoliation of ZnAl-LDH using NaOH/urea aqueous solution at low temperatures by taking advantage of a special property of alkali and urea aqueous solution systems at low temperatures that could easily intercalate into interlayer regions of LDH and attach on the host layers.[85] Fig. 9 illustrates the possible exfoliation mechanism that is proposed in their study. In 2018, O'Hare *et al.*[71] developed a new solvothermal post-synthesis treatment for preparing high aspect ratio MgAl-LDH. To be specific, as shown in Fig. 10, treating laurate-intercalated MgAl-LDH in pure ethanol using an autoclave was found to produce delaminated MgAl-LDH nanosheets with a thickness of ~2.6 nm. The authors reported that the high pressure solvothermal process promotes the insertion of ethanol molecules into the LDH interlayer space, thereby facilitating the exfoliation.

Although direct liquid phase exfoliation can avoid the drawback of conducting pre-treatment, this route not only possesses the same disadvantages as liquid phase exfoliation with pre-treatment but it also cannot be applied to all LDH.

2.1.3 Solid phase exfoliation. Up to now, several different methods belonging to solid phase exfoliation have been developed, such as solid phase exfoliation with the assistance of melting solid phase exfoliating material (SPEM), plasma-induced exfoliation, *etc.* Solid-state exfoliation with the assistance of SPEM is a highly-efficient, convenient, and environmentally-friendly solid-phase exfoliation technique and SPEM has the same effect as the used intercalation molecules or anions described in method 2.1.1. One typical example is that, in 2019, Li *et al.*[86] realized the successful exfoliation of CoAl-LDH with the assistance of a water-soluble

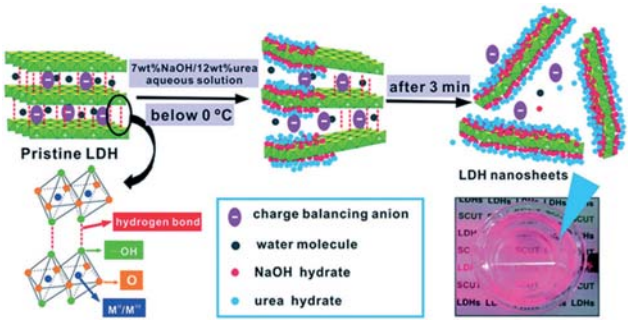

Fig. 9 Schematic diagram of exfoliation of LDH in precooled NaOH/urea aqueous solution. Reproduced with permission from ref. 85.

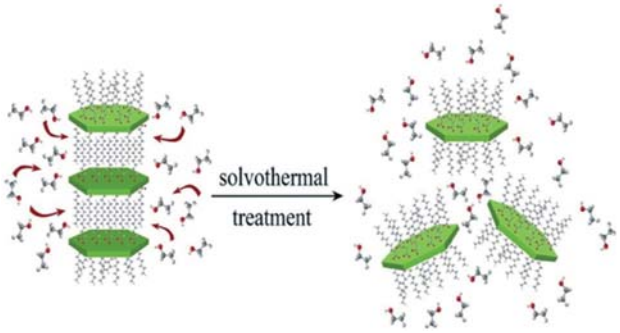

Fig. 10 Schematic representation of a new solvothermal post-synthesis treatment for the preparation of MgAl-LDH nanosheets. Reproduced with permission from ref. 71.

polymer. As shown in Fig. 11, the process involved employing a hydrothermal method to synthesize bulk CoAl-LDH, followed by adding the formed LDH into the molten water-soluble polymer at 60 °C in the open mill that can provide the shearing force. The ultrathin thickness of obtained LDH nanosheets was confirmed by AFM and the Tyndall effect.

Plasma-induced exfoliation is also applied as an efficient method for realizing solid phase exfoliation of LDH. The mechanism is that the utilized plasma can destroy the ionic bonds and hydrogen bonds in the interlayers of the bulk LDH, disturbing the normal charge balance and separating the positively charged brucite-like host layers from each other.[87] Wang *et al.*[87] pioneeringly exfoliated bulk CoFe-LDH into ultrathin LDH nanosheets with multiple vacancies through Ar plasma etching (Fig. 12). In their subsequent study,[88] the bulk CoFe-LDH were synthesized by a typical hydrothermal reaction, followed by treating the bulk CoFe-LDH *via* the N_2 plasma for 60 min. Interestingly, as presented in Fig. 13, they successfully realized not only the exfoliation of bulk CoFe-LDH into edge-rich ultrathin LDH nanosheets but also the nitrogen doping by N_2 plasma.

Compared to the liquid exfoliation of LDH, solid phase exfoliation is a process without involving costly and toxic solvents. Meanwhile, it can also avoid the adsorption of solvent molecules on the surface of obtained ultrathin nanosheets, decreasing the difficulty in the evaluation of intrinsic catalytic performance. However, developing a general method that can be applied to most LDH remains to be found.

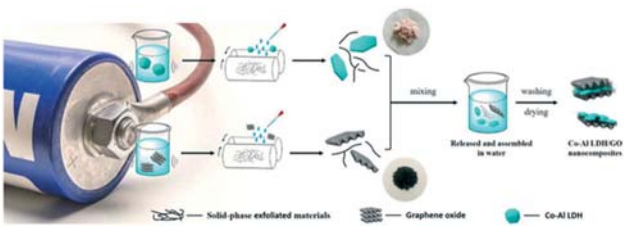

Fig. 11 Schematic illustration of the preparation of CoAl-LDH/GO nanocomposites. Reproduced with permission from ref. 86.

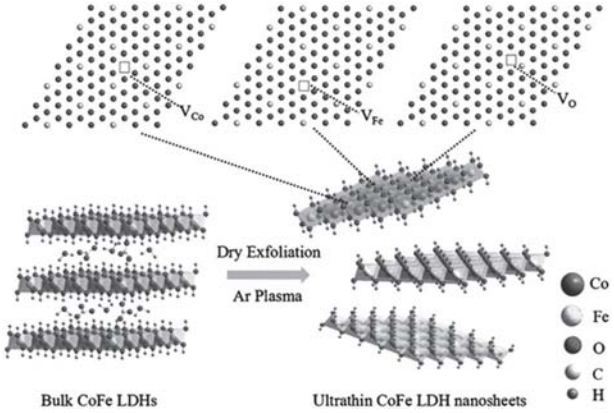

Fig. 12 CoFe-LDH nanosheets by Ar plasma exfoliation. Reproduced with permission from ref. 87.

2.2 Bottom-up approach

The bottom-up approach starts from suitably designed molecular precursors to build up 2D networks connected by chemical bonds *via* a chemical reaction. It is an attractive route for the production of 2D LDH because of its potential for mass production and facile preparation process. The typical synthesis strategies belonging to this approach are liquid phase synthesis without and with the assistance of external forces, corrosion engineering method, dry grinding, *etc.*

2.2.1 Liquid phase synthesis without the assistance of external forces. Liquid phase synthesis without the assistance of external forces is a widely used method for the production of LDH, which is carried out in a pure solvent or mixed solvents under operation at room temperature or higher temperature in a vacuum or atmospheric environment. One typical example is the hydrothermal/solvothermal synthesis method, which utilizes that the dissolved metal cations react with alkali solution under the condition of high temperature (100–1000 °C) and increased pressure in an airtight vessel. For instance, Yan *et al.*[89] reported one novel single-step approach to prepare large-scale LDH nanosheets in aqueous solution, and the synthesis process involves not only the growth of bulk LDH but also the spontaneous exfoliation. The procedures involve dissolving $Mg(NO_3)_2$, $Al(NO_3)_3$ and urea in 30 mL 30 wt% H_2O_2, followed by hydrothermal treatment at 150 °C for 24 h. The authors speculated that the successful exfoliation is determined by the rapid decomposition of H_2O_2 to generate a large amount of O_2 that resulted in violent movements of LDH layers. Yu *et al.*[90] synthesized a CoAl-LDH which stays stable in water and powdery state using ethylene glycol as a reaction medium. The synthesis is carried out as follows. Typically, $Co(NO_3)_2 \cdot 6H_2O$, $Al(NO_3)_3 \cdot 9H_2O$, and urea were dissolved in 80 ml of ethylene glycol, and the homogenous mixture solution was poured into a 100 ml Teflon-lined autoclave, and heated at 100 °C for 24 h. Note that the increased pressure is not necessary for the synthesis of LDH *via* liquid phase synthesis without the assistance of external forces, and obtaining LDH under normal atmospheric pressure is also possible. For example, Sun and coworkers[91] reported a quick synthesis (10 min) of MgAl-LDH single-layer nanosheets at 80 °C in the presence of formamide (23 vol%). The authors found that the presence of formamide is necessary for the formation of LDH single-layer nanosheets. Based on comprehensive investigations, as shown in Fig. 14, they expected that formamide molecules can adhere to the LDH sheet surface during the growth process, thus preventing the interlayer growth. Besides, Sun *et al.*[92] realized the synthesis of MgAl-LDH single-layer nanosheets through a single-step process in the presence of formamide, namely titrating an aqueous solution containing $Mg(NO_3)_2$ and $Al(NO_3)_3$ into sodium hydroxide solution in the presence of 2.0, 5.0, 15.0, or 30.0 vol% formamide. Yang *et al.*[93] prepared unilamellar MgAl-LDH nanosheets *via* rapidly mixing formamide containing $Mg(NO_3)_2 \cdot 6H_2O/Al(NO_3)_3 \cdot 9H_2O$ and formamide containing NaOH. Hou *et al.*[94] developed a simple aqueous synthetic route to prepare MgAl-LDH, and the synthesis route includes adding the mixed salt solution and $NH_3 \cdot H_2O$ solution (7 wt%) simultaneously to a beaker within ~10 min under magnetic stirring and N_2 protection. During this process, the pH of the reaction system was held at ~10 by controlling the relative addition rates of the two raw material solutions. Moreover, Hu *et al.*[95] report a facile one-step synthesis of LDH monolayers in a reverse microemulsion, which involves introducing the traditional aqueous co-precipitation system

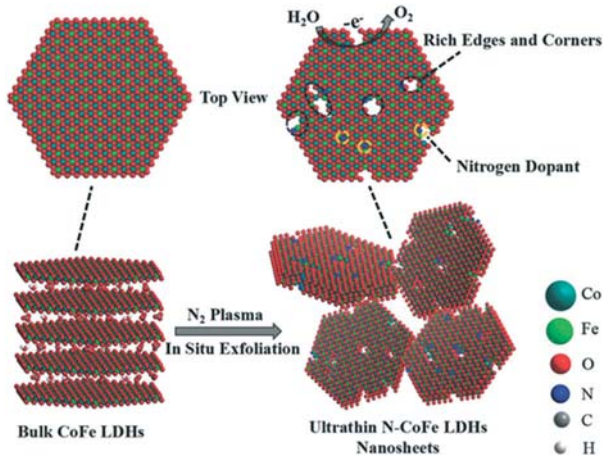

Fig. 13 Illustration of the exfoliation of bulk CoFe-LDH into ultrathin CoFe-LDH nanosheets by N_2 plasma. Reproduced with permission from ref. 88.

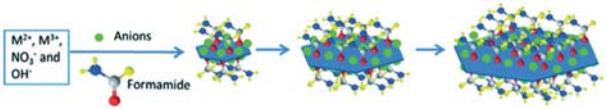

Fig. 14 Schematic representation of the direct growth of single-layer nanosheets in formamide solution. Reproduced with permission from ref. 91.

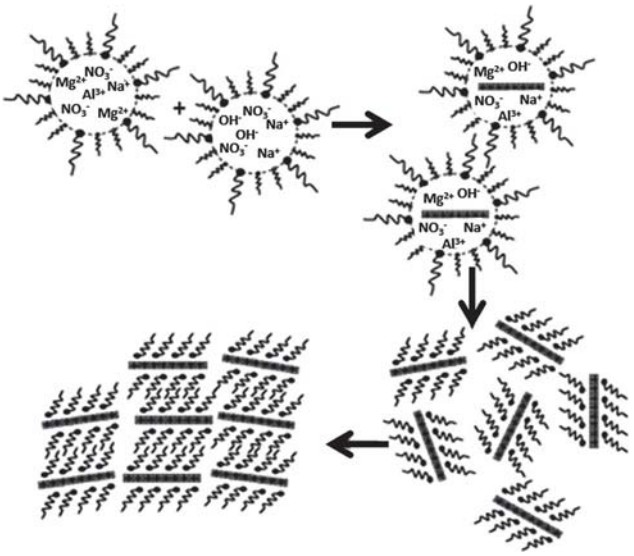

Fig. 15 Schematic representation of the nucleation and growth of LDH platelets. Reproduced with permission from ref. 95.

into an oil phase of isooctane with sodium dodecyl sulfate as surfactant and 1-butanol as co-surfactant. The formation mechanism of LDH monolayers can be attributed to the following condition. As shown in Fig. 15, aqueous droplets containing the reactants were surrounded by DS^- groups in the oil phase. These droplets acted as nanoreactors to confine space and nutrients for the growth of LDH platelets, providing a way to control the size of the LDH platelets both in diameter and thickness. Pang *et al.* realized the preparation of Mg_2Al–NO_3^--LDH nanosheets dispersed in aqueous media without using any surfactants. The experiment was carried out at room temperature by pumping a mixed salt solution containing Mg^{2+}/Al^{3+} cations and a diluted $NH_3{\cdot}H_2O$ solution into the T-type microchannel reactor through two inlets. AFM was used to characterize the exact thickness of the obtained ultrathin nanosheets and the results confirm the fact that the resulting LDH nanosheets were of a thickness of *ca.* 0.68–1.13 nm.[96]

Note that the synthesis methods belonging to liquid phase synthesis without the assistance of external forces vary from one system to the other, which is disadvantageous for the development of a universal synthesis method. In addition, these reported methods possess low controllability of thickness and size.

2.2.2 Liquid phase synthesis with the assistance of external forces. Different external forces have been applied to facilitate liquid phase synthesis of LDH. A typical example is that Müller *et al.*[97] synthesized a series of NiFe-LDH nanosheets with different interlayer anions *via* pulsed-laser ablation in liquids (PLAL). Preparing nanoparticles *via* PLAL mainly depends on the very rapid cooling of a plasma comprised of elements from the solid ablation target and the surrounding liquid.[98] Besides, using microwaves as an energy source for the synthesis of LDH has been extensively investigated during recent years.[99–101] For instance, Qiao *et al.*[102] reported a one-step microwave-assisted approach for the preparation of ultrathin and porous ZnCo-LDH nanosheets, and such approach has some advantages, including high yield and simple synthesis. Moreover, the electrodeposition method is also an effective means to generate LDH *via* adjusting an external power source to activate the reaction.[103] One example is that Scavetta *et al.*[104] have successfully synthesized CoAl-LDH by the cathodic reduction of a 0.03 M Co and Al nitrate solution. The thickness and Co/Al ratios can be tuned by simply changing the electrolytic bath composition and the electrosynthesis length. Recently, Yan *et al.* reported a facile ultrasonication-assisted methodology to eco-friendly synthesize NiCo-LDH and NiFe-LDH nanosheets.[105,106] The authors found that using ultrasonication is beneficial for the formation of ultrathin structures and the absence of ultrasonic treatment leads to the formation of bulky LDH. Other than the above-mentioned external forces, the mechanical force is also a common way that can be utilized before or during liquid phase synthesis to facilitate the formation of LDH.[107] For example, as presented in Fig. 16, Zhang *et al.*[108] obtained Mg_2Al–NO_3^--LDH with high crystallinity and good dispersity *via* grinding MgO and Al_2O_3 (ball mill) followed by hydrothermal treatment at 353 K for 6 h in $NaNO_3$ solution. Iwasaki *et al.*[109] presented a single-step wet grinding to produce iron-based LDH by adding $CoCl_2$ solution into a milling pot and milling with steel balls. A possible formation route was proposed by the authors as follows: substitution reaction between H_2O and Fe component from the steel balls providing the iron source and the OH^- for the precipitation of the LDH phase. Very recently, Song *et al.*[110] utilized a separate nucleation and aging step method based on a commercial colloidal mill reactor to realize the scale-up preparation of a series of ultrathin MgAl-LDH, CoAl-LDH, NiCo-LDH, and NiFe-LDH. Note that the authors introduced a small amount of the layer growth inhibitor formamide in the synthesis process. Subsequently, they developed a method for the scaled-up synthesis of the series of monolayer LDH without the addition of organic solvents *via* a separate nucleation and aging step process based on a commercial colloidal mill reactor.[111]

2.2.3 Corrosion engineering method. Apart from the conventional liquid phase synthesis methods mentioned above, the corrosion engineering method, in which one kind of metal cations was provided by pure metal instead of metallic salt, is a newly developed method for the

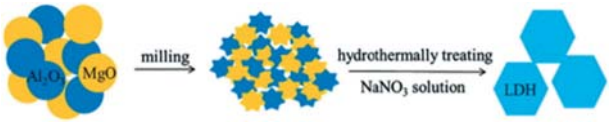

Fig. 16 Schematic representation of synthesizing Mg_2Al–NO_3^--LDH *via* the mechano-hydrothermal method. Reproduced with permission from ref. 108.

preparation of LDH. Since the corrosion engineering method is usually conducted in aqueous solution at room temperature, it is regarded as an energy-efficient and cost-effective method. One typical example is that, as shown in Fig. 17, Liu *et al.*[112] reported that different Fe-based LDH can be generated by immersing iron substrates (*e.g.*, iron plate) in an aqueous solution containing a certain amount of divalent cations (*e.g.*, Ni^{2+}, Co^{2+}, Mn^{2+}, or Mg^{2+}) at ambient temperature. Note that, among these obtained LDH, NiFe-LDH nanosheet arrays on iron substrate deliver remarkable oxygen evolution catalytic activities and excellent durability for over 6000 h at a high current density of 1000 mA cm^{-2}. Besides, Fu *et al.* constructed porous NiFe-LDH with rich edge/surface-Fe defects on Ni foam *via* an elaborate atmosphere corrosion strategy, and such strategy involves two steps, the liquid etching for loading Fe source and the subsequent atmosphere corrosion for NiFe-LDH formation.[113]

2.2.4 Dry grinding. Dry grinding *via* ball milling or manual grinding is a solid phase bottom-up synthesis method without the involvement of solvent, which usually involves two steps in sequence. The first step is activating the hydroxide or metallic salts to form a weakened crystal structure *via* the grinding operation, and the second step is the washing operation that can offer the required crystal water to form LDH. For example, Khusnutdinov *et al.*[114] prepared MgAl-LDH with a small amount of $Mg(OH)_2$ for the Mg/Al molar ratio from 3/1 to 6/1 *via* grounding $Mg(OH)_2$ and $AlCl_3{\cdot}6H_2O$ in a planetary mill and washing the activated products. Later on, Mafra *et al.*[115] successfully generated hydrotalcite-like MgAl–NO_3^--LDH in a mortar by manually grinding the hydrated magnesium and aluminum nitrate salts with sodium hydroxide. Note that, although this approach possesses the potential to overcome the difficulties related to solution operation, such as the different rates of precipitation with pH regulation, only several LDH systems have been successfully generated by this way. Besides, the thickness/lateral size controllability remains to be improved through this method.

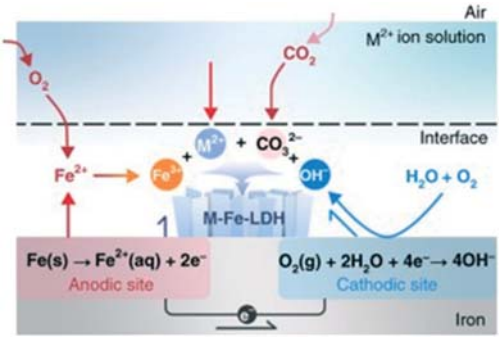

Fig. 17 Schematic illustrations of the formation and microstructure of Fe-based LDH on the surface of iron substrates. Reproduced with permission from ref. 112.

2.3 Decomposition-regrowth strategy

Decomposition-regrowth strategy, which relies on the decomposition of original nanomaterials and the regrowth of LDH,[116–118] can be regarded as a special method that belongs to bottom-up approach based on the fact that such a strategy requires not only molecular precursors but also the already formed nanomaterials.

The ion/atom exchange method is one typical example that belongs to the decomposition-regrowth strategy. On the one hand, the original nanomaterials can be LDH. For instance, Mourid *et al.* prepared ZnAl-2,4,5-trichlorophenoxyacetic acid-LDH *via* replacing chloride ions of ZnAl–Cl-LDH, which is realized by stirring an aqueous solution containing the LDH phase and the anion to be inserted.[119] On the one hand, the original nanomaterials can be other materials for the ion/atom exchange method. For example, Bai *et al.*[120,121] successfully realized the transformation of ZIF-67 to CoCo-LDH and NiCo-LDH *via* a fast ion-exchange process that is illustrated in Fig. 18. Besides, on the bias of operando X-ray spectroscopy combined with *ex situ* characterization, Su *et al.*[122] demonstrated that NiFe Prussian blue analogues could be entirely transformed into the amorphous Fe-doped $Ni(OH)_2$ structure after the electrocatalysis activation process. Furthermore, Xu *et al.*[123] presented an ingenious one-step reaction strategy to fabricate NiFeCe-LDH microcapsules by taking Ce-doped MIL-88A as a precursor (Fig. 19).

Apart from the ion/atom exchange method, Chen *et al.*[124] reported a novel *in situ* exfoliation method driven by Ostwald ripening to produce ultrathin LDH nanosheets on the conductive electrodes by spontaneously self-etching and redepositing *via* a simple hydrothermal treatment without

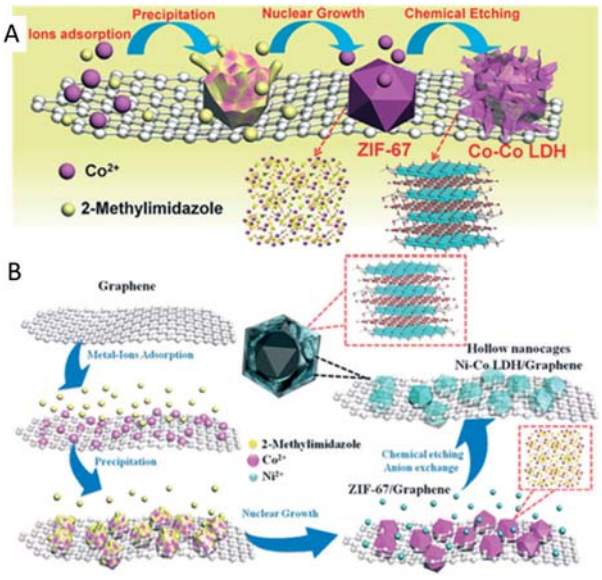

Fig. 18 (A) Illustration of the fabrication procedure of CoCo-LDH hollow nanocages/graphene. (B) Schematic illustration of the synthesis procedure of the NiCo-LDH hollow nanocages/graphene composite. Reproduced with permission from ref. 120 and 121.

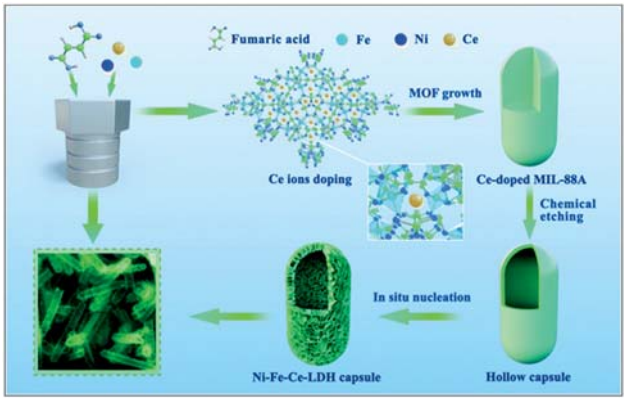

Fig. 19 Schematic illustration of the fabrication of hollow Ni–Fe–Ce-LDH microcapsules mediated by cerium doping in MIL-88A. Reproduced with permission from ref. 123.

the assistance of exfoliating reagent (Fig. 20), while Miyata *et al.*[125] reported that the metal oxide derived from calcined hydrotalcite can be hydrated to reconstruct the structure of LDH in anion solution due to the memory effect of hydrotalcite. Besides, as shown in Fig. 21, Qin *et al.*[126] presented that $Co(OH)_2$ nanoplates can convert to CoCo-LDH by magnetical shaking hundreds of milligrams of $Co(OH)_2$ that was dispersed in a solution containing Br_2 and acetonitrile for one day at room temperature, because of the single-crystal property, namely, an oxidative intercalation process based on redox-able transition-metal elements.

Despite enormous progress in the development of the decomposition-regrowth strategy, we have to admit that this strategy is only compatible with the systems that possess the suitable precursor, thereby impeding its generalization.

3. Important parameters relating to the synthesis process and the obtained products of different synthesis methods

The production cost, which is strongly associated with the synthesis process, and the quality of the final products are

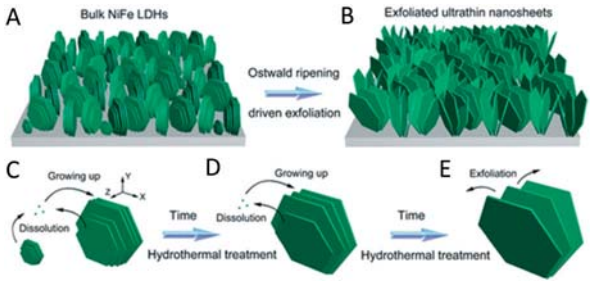

Fig. 20 Schematic for the Ostwald ripening driven exfoliation of pristine bulk NiFe-LDH into exfoliated ultrathin nanosheets. (A) Bulk NiFe-LDH on the Cu electrode. (B) Ultrathin NiFe-LDH nanosheets. (C–E) Schematic illustrations to show the ORDE process. Reproduced with permission from ref. 124.

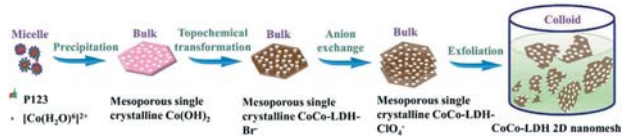

Fig. 21 The schematic of the synthesis process of CoCo-LDH 2D nanomesh. Reproduced with permission from ref. 126.

two key factors that affect the practical application of 2D LDH. Therefore, several important parameters relating to the synthesis process and the obtained products of different synthesis methods are summarized in Table 1. We hope this table can act as a platform that will help researchers to easily understand the advantages and disadvantages of the existing synthesis routes, which is beneficial for selecting a suitable synthesis method according to the desired characteristics of the synthesis process and the obtained products.

4. Some current challenges and further tasks

Although a great number of studies have been performed to explore the synthesis of LDH and enormous progress in this field has been made, the further development and effective utilization of LDH still involve many challenges. Presenting current challenges and further tasks regarding the synthesis of LDH is highly needed for understanding the direction for future efforts. However, insufficient attention has been given to this topic in previous reports. Accordingly, in this section, we listed some current challenges and further tasks regarding the preparation of LDH.

1, Although advance in the area of preparing LDH has been promoted by the development of various synthesis strategies, these existing strategies vary from one system to the other, prohibiting a universal synthesis strategy. Meanwhile, current synthesis comes with at least one of the following technical drawbacks: the high cost (special equipment, expensive reactants), tedious operation (post-treatment, multi-step operation), eco-unfriendly conditions (non-green organic solvents) and the possible contamination caused by organic molecule adsorption. Therefore, more focused efforts are required to develop new synthesis strategies that can overcome these challenges associated with these existing strategies.

2, It is well known that the property of an LDH material is strongly dependent on its thickness and lateral size. For instance, compared with bulk LDH, ultrathin atomically scaled or single-unit cell-thick LDH nanosheets (NSs) have shown enhanced catalytic performance because of their improved intrinsic catalytic activity and electronic conductivity.[127] Thus, it would be necessary to optimize the synthesis route and to realize the synthesis of 2D LDH nanosheets with controllable thickness and lateral size.

3, Liquid phase synthesis and liquid phase exfoliation are the most widely used methods for preparing LDH.[9] However, the agglomeration or re-staking of ultrathin LDH

Table 1 Important parameters relating to the synthesis process and the obtained products of different synthesis methods

No.	Nanomaterials	Production method	Production process (used device + reaction temperature (T) + reaction pressure (P))	Reagents	Yield	Crystallinity	Lateral size and thickness	Ref.
1	ZnAl-LDH	Liquid phase exfoliation with pre-treatment	1, The synthesis of precursor by the coprecipitation method (flask + 25 °C + 1 atm) 2, Intercalation of dodecyl sulfate (DS) (flask + 25 °C + 1 atm) 3, Dispersion of [Zn_2Al-DS] in solvent under reflux conditions (reflux setup + 120 °C + 1 atm)	Zinc chloride Aluminum chloride Sodium hydroxide Sodium dodecyl sulfate Butanol	1 g	High	140 nm/no data	65
2	LiAl-LDH	Liquid phase exfoliation with pre-treatment	1, The synthesis of precursor by the coprecipitation method (beaker + 90 °C + 1 atm) 2, Intercalation of surfactant (beaker + 25 °C + 1 atm) 3, Dispersion of surfactant-LDH in solvent under reflux conditions (reflux setup + 120 °C + 1 atm)	Gibbsite Lithium salts Sodium dodecyl sulfate Butanol	1 g	High	1 and 5 μm/no data	66
3	FeCo-LDH	Liquid phase exfoliation with pre-treatment	1, The synthesis of precursor *via* a hydrothermal method (autoclave + 120 °C + high pressure) 2, Exfoliation of precursor induced by graphdiyne (three-necked bottle + 50 °C/Ar + 1 atm)	Cobalt nitrate urea Ferrous chloride ammonium fluoride Ethanol Acetone Pyridine Tetramethylethylenediamine Hexaethynylbenzene	No data	High	0.5 μm/7 nm	70
4	MgAl-LDH	Liquid phase exfoliation with pre-treatment	1, The synthesis of the precursor by the coprecipitation and homogeneous precipitation method (beaker + 80 °C + 1 atm) 2, Pre-treatment *via* the urea reflux method (reflux setup + 140 °C + 1 atm) 3, Exfoliation by the solvothermal post-synthesis treatment (autoclave + 150 °C + high pressure)	Magnesium nitrate Aluminum nitrate Lauric acid Sodium hydroxide Urea Ethanol	0.5 g	High	200 nm −1 μm/2.6 nm	71
5	MgAl-LDH	Liquid phase exfoliation with pre-treatment	1, The synthesis of the precursor by the hydrothermal method (autoclave + 140 °C + high pressure) 2, Pre-treatment of precursor (vessel + 25 °C/N_2 + 1 atm) 3, Exfoliation by shaking the aqueous solution containing $NaNO_3$, HNO_3 and precursor (flask/mechanical shaker + 25 °C + 1 atm)	Magnesium nitrate Aluminum nitrate hexamethylenetetramine Sodium nitrate Nitric acid Formamide	0.05 g	High	>1 μm/0.8 nm	72
6	MgAl-LDH	Liquid phase exfoliation with pre-treatment	1, The synthesis of the precursor by the coprecipitation method (beaker + 25 °C/N_2 + 1 atm) 2, Intercalation of surfactant (beaker + 25 °C + 1 atm) 3, Exfoliation by stirring the precursor in toluene (beaker + 25 °C + 1 atm)	Magnesium nitrate Aluminum nitrate Ammonia solution Sodium dodecyl sulfate Toluene	Around hundreds of mg	High	1 μm/3 nm	67
7	MgAl-LDH	Liquid phase exfoliation with pre-treatment	1, The synthesis of the precursor by the hydrothermal method (autoclave + 140 °C + high pressure) 2, Intercalation of surfactant (reflux setup + 45 °C/N_2 + 1 atm) 3, Exfoliation in a micro-reactor microreactor in the presence of absolute ethanol	Magnesium nitrate Aluminum nitrate Urea Methanol Glacial acetic acid Sodium dodecyl sulfate	0.3 g	High	500 nm – several μm/2–4 nm	68

Table 1 *(continued)*

No.	Nanomaterials	Production method	Production process (used device + reaction temperature (T) + reaction pressure (P))	Reagents	Yield	Crystallinity	Lateral size and thickness	Ref.
8	ZnCr-LDH	Direct liquid phase exfoliation	1, The synthesis of ZnCr-LDH by direct coprecipitation (beaker + 25 °C + 1 atm) 2, Exfoliation of ZnCr-LDH by vigorous shaking of LDH sample in the formamide under N_2 bubbling (beaker + 25 °C/N_2 + 1 atm)	Zinc chloride Aluminum chloride sodium hydroxide Formamide	1 g	High	50 nm/no data	75
9	FeNi-LDH	Direct liquid phase exfoliation	1, The synthesis of the precursor by the hydrothermal method (Teflon-lined stainless steel + 120/160 °C + high pressure) 2, Exfoliation in Ar purged formamide under vigorous stirring (beaker + 25 °C/Ar + 1 atm)	Nickel acetate Iron(III) nitrate *N*,*N*-Dimethylformamide Formamide	15 mg	High	100 nm/1 nm	76
10	NiMn-LDH	Direct liquid phase exfoliation	1, The synthesis of the precursor by the hydrothermal method (Teflon-lined stainless steel + 180 °C + high pressure) 2, Exfoliation in Ar purged formamide under vigorous stirring (beaker + 70 °C/N_2 + 1 atm)	Nickel nitrate Manganese chloride Methanol Formamide	0.1 g	High	50 nm/1–3 nm	77
11	MgAl-LDH	Direct liquid phase exfoliation	1, The synthesis of the precursor by the coprecipitation method (beaker + 60 °C/N_2 + 1 atm) 2, Exfoliation by ultrasonic treatment (screw-capped test tube + 25 °C + 1 atm)	Aluminum chloride Magnesium chloride Sodium dodecyl sulfate Potassium hydroxide CCl_4 or toluene	0.4 g	No data	No data	79
12	CoFe-LDH	Liquid phase exfoliation with pre-treatment	1, The synthesis of lactate–intercalated CoFe-LDH by hydrothermal method (autoclave + 60 °C + high pressure) 2, Preparation of exfoliated nanosheet *via* laying aside without any treatment (round-bottom flask + 25 °C + 1 atm)	DL-Lactic acid Iron powder Hydrogen peroxide Cobalt powder Sodium hydroxide	Around hundreds of mg	High	Less than 100 nm/1–2 nm	81
13	ZnAl-LDH	Direct liquid phase exfoliation	1, The synthesis of brucite-like ZnAl-LDH *via* the urea hydrolysis method (reflux setup + 105 °C + 1 atm) 2, Exfoliation of ZnAl-LDH using NaOH/urea aqueous solution at low temperature (beaker + −10 °C + 1 atm)	Zinc chloride Aluminum chloride Urea Sodium hydroxide	Around 10 g	Low	50 nm/0.6 nm	85
14	MgAl-LDH	Direct liquid phase exfoliation	1, The synthesis of the precursor by co-precipitation under inert conditions (beaker + 60 °C/N_2 + 1 atm) 2, Exfoliation *via* an ultrasonic water bath in formamide (beaker/ultrasonic setup + 25 °C + 1 atm)	Magnesium nitrate Aluminum nitrate Potassium hydroxide Formamide	Around 10 g	No data	20–40 nm/2–4 nm	83
15	CoAl-LDH	Direct liquid phase exfoliation	1, The synthesis of the precursor by a reflux method (reflux setup + 97 °C/Ar + 1 atm) 2, Direct exfoliation *via* a tip sonication approach (horn-probe sonic tip + cooling + 1 atm)	Cobalt chloride Aluminum chloride Urea Different organic solvents	20 mg	High	400 nm/3–6 nm	78
16	FeNi-LDH	Direct liquid phase exfoliation	1, The synthesis of the precursor by the hydrothermal method (Teflon-lined stainless steel + 120 °C + high pressure) 2, Exfoliation using an ultrasonic processor (ultrasonic processor + 25 °C + 1 atm)	Iron(III) chloride Nickel nitrate Urea	No data	High	200 nm/16–20 nm	82

Table 1 *(continued)*

No.	Nanomaterials	Production method	Production process (used device + reaction temperature (T) + reaction pressure (P))	Reagents	Yield	Crystallinity	Lateral size and thickness	Ref.
17	CoAl-LDH	Solid phase exfoliation	1, The synthesis of precursor by the hydrothermal method (Teflon-lined stainless steel + 120 °C + high pressure) 2, Solid phase exfoliation (open mill + 60 °C + 1 atm)	Cobalt nitrate Aluminum nitrate Ammonium fluoride Urea Solid phase materials	Around 1 g	High	1 μm/around 2 nm	86
18	CoFe-LDH	Solid phase exfoliation	1, The synthesis of the precursor by the hydrothermal method (Teflon-lined stainless steel + 80 °C + high pressure) 2, Solid phase exfoliation (plasma reactor + 25 °C/Ar + 0.2–0.4 Pa)	Iron(III) nitrate Cobalt nitrate Sodium hydroxide Sodium carbonate	20 mg	High	100 nm/0.6 nm	87
19	CoFe-LDH	Solid phase exfoliation	1, The synthesis of the precursor by the hydrothermal method (Teflon-lined stainless steel + 80 °C + high pressure) 2, Solid phase exfoliation (plasma reactor + 25 °C/N_2 + 1 atm)	Iron(III) nitrate Cobalt nitrate Sodium hydroxide Sodium carbonate	20 mg	High	200 nm/1.6 nm	88
20	MgAl-LDH	Liquid phase synthesis without the assistance of external forces	Direct synthesis of LDH ultrathin nanosheets by coprecipitation (beaker + 80 °C + 1 atm)	Magnesium nitrate Aluminum nitrate Sodium nitrate Formamide Sodium hydroxide	Around 50 mg	High	30 nm/0.8 nm	91
21	MgAl-LDH	Liquid phase synthesis without the assistance of external forces	Direct synthesis of LDH ultrathin nanosheets *via* the hydrothermal method (Teflon-lined stainless steel + 150 °C + 12.6 MPa)	Magnesium nitrate Aluminum nitrate Urea Hydrogen peroxide	Around 0.15 g	High	100 nm/0.44 nm	89
22	MgAl-LDH	Liquid phase synthesis without the assistance of external forces	Direct synthesis of LDH ultrathin nanosheets by coprecipitation (T-type microreactor + 25 °C + 1 atm)	Magnesium nitrate Aluminum nitrate Ammonia solution	Around 1 g	High	20–30 nm/0.68–1.13 nm	96
23	FeNi-LDH	Liquid phase synthesis with the assistance of external forces	Direct synthesis of LDH ultrathin nanosheets by pulsed laser ablation in liquids (pulsed laser ablation in liquids + 25 °C + 1 atm)	Iron powder Nickel salt	Around gram scale	High	No data	97
24	CoAl-LDH	Liquid phase synthesis with the assistance of external forces	Microwave-assisted direct synthesis of LDH ultrathin nanosheets (reflux setup/microwave reactor + 100 °C + 1 atm)	Cobalt nitrate Aluminum nitrate Urea	Around gram scale	High	1 μm/no data	99
25	ZnAl-LDH	Liquid phase synthesis with the assistance of external forces	Direct synthesis of LDH ultrathin nanosheets by electrodeposition method (potentiostat + 25 °C + 1 atm)	Alloy sheet Zinc nitrate Aluminum nitrate	No data	High	No data	103
26	MgAl-LDH	Liquid phase synthesis with the assistance of external forces	1, The production of precursor *via* calcination treatment (muffle oven + 550 °C + 1 atm) 2, Milling the mixture of MgO and Al_2O_3 (ball mill + 25 °C + 1 atm) 3, Hydrothermal treatment (Teflon-lined stainless-steel autoclave + 80 °C + high pressure)	Magnesium nitrate Aluminum hydroxide Sodium nitrate	Around gram scale	High	280 nm/3.3 nm	108
27	CoFe-LDH	Liquid phase synthesis with the assistance of external forces	Direct synthesis of LDH ultrathin nanosheets by mechanochemical process (ball mill + 25 °C/Ar + 1 atm)	Cobalt chloride Carbon steel balls	Around gram scale	High	284 nm/no data	109

Table 1 *(continued)*

No.	Nanomaterials	Production method	Production process (used device + reaction temperature (T) + reaction pressure (P))	Reagents	Yield	Crystallinity	Lateral size and thickness	Ref.
28	NiFe-LDH	Liquid phase synthesis with the assistance of external forces	Direct synthesis of LDH ultrathin nanosheets *via* rapid mixing and nucleation in a colloid mill without further aging (colloid mill + 25 °C/Ar + 1 atm)	Iron(III) nitrate Nickel nitrate Formamide Sodium hydroxide	0.3 g/2 min	Low	15 nm/0.8 nm	110
29	FeNi-LDH	Corrosion engineering method	Direct synthesis of LDH ultrathin nanosheets by corrosion engineering method (flask + 25 °C + 1 atm)	Nickel sulfate Iron plate	No data	Low	No data/8 nm	112
30	MgAl-LDH	Dry grinding	Direct synthesis of LDH ultrathin nanosheets by mechanochemical process (planetary ball mill + 25 °C + 1 atm)	Magnesium hydroxide Aluminum chloride	No data	High	No data	114
31	CoCo-LDH	Ion/atom exchange strategy	1, The synthesis of ZIF-67 (beaker + 25 °C + 1 atm) 2, The production of LDH nanosheets *via* ion/atom exchange strategy (reflux setup + 25 °C + 1 atm)	Cobalt nitrate 2-Methylimidazole Methanol Ethanol	Around half gram	Low	No data	120
32	FeNi-LDH	Ion/atom exchange strategy	1, The synthesis of MIL-88A particles (Teflon-lined stainless autoclave + 110 °C + high pressure) 2, The synthesis of hollow FeNi-LDH hollow microcapsules (water bath + 90 °C + 1 atm)	Fumaric acid Iron(III) nitrate Ethanol Nickel nitrate Urea	Around hundreds of mg	Low	Around hundreds of nm/no data	123
33	FeNi-LDH	*In situ* exfoliation strategy driven by Ostwald ripening	1, The synthesis of bulk NiFe-LDH on the Cu mesh (Teflon--lined stainless steel autoclave + 120/160 °C + high pressure) 2, Ostwald ripening driven exfoliation of NiFe-LDH *in situ* on Cu mesh (Teflon-lined stainless steel autoclave + 160 °C + high pressure)	Nickel nitrate Iron(III) nitrate *N*,*N*-Dimethylformamide	No data	High	Around 1 μm/4–9 nm	124
34	CoCo-LDH	Topochemical method	1, The synthesis of $Co(OH)_2$ (water bath + 80 °C + 1 atm) 2, The synthesis of CoCo-LDH nanomesh (vessel + 25 °C + 1 atm)	Pluronic P123 Cobalt nitrate Ammonia solution Bromine Acetonitrile	Around hundreds of mg	High	Around hundreds of nm/no data	126

nanosheets after collecting the product from the reaction solvent is an inherent issue. For instance, Yu *et al.*[91] reported that the synthesized monolayer MgAl-LDH nanosheets tend to re-stack when this dispersion sample was cast and dried onto a silicon wafer. The process of agglomeration or re-staking may be caused by physical entanglement, electrostatic interactions, or high surface energy of ultrathin nanosheets. Because the change of thickness has a substantial effect on the performance of ultrathin nanosheets in relevant fields, it is highly desirable to resolve this challenge by improving the preparation condition of corresponding LDH.

4, Mass production of a material is one of the prerequisites for realizing its industrial application. However, the yields of existing synthesis methods for LDH range mostly from milligrams to grams, which cannot meet the needs for practical application. This challenge has motivated the need for developing new synthesis methods that can realize the mass production of desirable 2D LDH.

5, It is well acknowledged that defect engineering is one effective strategy to enhance the performance of LDHs since the structural defect can dramatically change the local chemical coordination and surface valence states of LDH.[22,128] Ultrathin or monolayer LDH prepared by different preparation methods will inevitably have defective structures, which is beneficial for conducting defect engineering of LDH. However, how to control the synthesis conditions to effectively realize the regulation of defective structures is still very challenging and difficult.

6, Recently, constructing LDH/other 2D material heterostructures with face-to-face contact (*e.g.* sheet-on-sheet and layer-by-layer) has been considered as an effective way to enhance the performance of LDH for the target application. Although some progress has been made in this field,[129–134] we still need to pay attention to realizing the customized, low-cost and easy preparation of such materials.

5. Summary

In this review, we systematically summarized various preparation methods of 2D LDH, including top-down approach, bottom-up approach, and decomposition-regrowth strategy, offering an overview of the possible synthesis routes. Besides, we listed several important parameters relating to both the synthesis process and the obtained products of various synthesis methods, such as the synthesis temperature/pressure, the used device, the utilized reactants, the presence or absence of pre/post-treatment, the yield, the crystallinity and the lateral size and thickness. We hope this table can act as a platform that can help researchers easily understand the advantages and disadvantages of the existing synthesis routes, which is beneficial for selecting a suitable synthesis method according to the desired characteristics of the synthesis process and the obtained products. Finally, some current challenges and further tasks regarding the synthesis of LDH are also presented, including the improvement of existing strategies, thickness/lateral size-controllable preparation, the agglomeration or re-staking of ultrathin LDH nanosheets and mass production, which are expected to encourage us to further improve the synthesis conditions of 2D LDH.

Author contributions

Z. Chen and Q. Fan contributed equally. The manuscript was written through contributions of all authors. All authors have given approval to the final version of the manuscript.

Conflicts of interest

The authors declare no competing financial interest.

Acknowledgements

This work was financially supported by the Sino-German Center for Research Promotion (Grants GZ 1351), the Deutsche Forschungsgemeinschaft DFG within the framework of the collaborative research center SFB-1214 project B1 and the National Natural Science Foundation of China (21775142).

Notes and references

1 J. Yu, Q. Wang, D. O'Hare and L. Sun, *Chem. Soc. Rev.*, 2017, **46**, 5950–5974.
2 S. Mallakpour, M. Hatami and C. M. Hussain, *Adv. Colloid Interface Sci.*, 2020, **283**, 102216.
3 F. Zhang, L. Zhao, H. Chen, S. Xu, D. G. Evans and X. Duan, *Angew. Chem.*, 2008, **120**, 2500–2503.
4 D. N. Ahmed, L. A. Naji, A. A. Faisal, N. Al-Ansari and M. Naushad, *Sci. Rep.*, 2020, **10**, 2042.
5 J. Shin, K. Kim and J. Hong, *Coatings*, 2020, **10**, 669.
6 Z. Z. Yang, C. Zhang, G. M. Zeng, X. F. Tan, H. Wang, D. L. Huang, K. H. Yang, J. J. Wei, C. Ma and K. Nie, *J. Mater. Chem. A*, 2020, **8**, 4141–4173.
7 S. Hao, G. Zheng, S. Gao, L. Qiu, N. Xu, Y. He, L. Lei and X. Zhang, *ACS Sustainable Chem. Eng.*, 2019, **7**, 14361–14367.
8 G. Fan, F. Li, D. G. Evans and X. Duan, *Chem. Soc. Rev.*, 2014, **43**, 7040–7066.
9 L. Lv, Z. Yang, K. Chen, C. Wang and Y. Xiong, *Adv. Energy Mater.*, 2019, **9**, 1803358.
10 A. R. Sotiles, L. M. Baika, M. T. Grassi and F. Wypych, *J. Am. Chem. Soc.*, 2018, **141**, 531–540.
11 J. Zhang, J. Liu, L. Xi, Y. Yu, N. Chen, S. Sun, W. Wang, K. M. Lange and B. Zhang, *J. Am. Chem. Soc.*, 2018, **140**, 3876–3879.
12 F. Dionigi, J. Zhu, Z. Zeng, T. Merzdorf, H. Sarodnik, M. Gliech, L. Pan, W. X. Li, J. Greeley and P. Strasser, *Angew. Chem.*, 2021, **60**, 8976–8982.
13 D. Wang, Q. Li, C. Han, Q. Lu, Z. Xing and X. Yang, *Nat. Commun.*, 2019, **10**, 1–12.
14 K. He, T. Tadesse Tsega, X. Liu, J. Zai, X. H. Li, X. Liu, W. Li, N. Ali and X. Qian, *Angew. Chem., Int. Ed.*, 2019, **58**, 11903–11909.

15 X. Zhang, Y. Zhao, Y. Zhao, R. Shi, G. I. Waterhouse and T. Zhang, *Adv. Energy Mater.*, 2019, **9**, 1900881.
16 J. Kang, X. Qiu, Q. Hu, J. Zhong, X. Gao, R. Huang, C. Wan, L. M. Liu, X. Duan and L. Guo, *Nat. Catal.*, 2021, **4**, 1050–1058.
17 Y. Zhao, L. Zheng, R. Shi, S. Zhang, X. Bian, F. Wu, X. Cao, G. I. Waterhouse and T. Zhang, *Adv. Energy Mater.*, 2020, **10**, 2002199.
18 L. Cao, Y. Ma, A. Song, L. Bai, P. Zhang, X. Li and G. Shao, *Int. J. Hydrogen Energy*, 2019, **44**, 5912–5920.
19 F. Song and X. Hu, *Nat. Commun.*, 2014, **5**, 4477.
20 J. Zhang, L. Yu, Y. Chen, X. F. Lu, S. Gao and X. W. Lou, *Adv. Mater.*, 2020, **32**, 1906432.
21 G. Chen, T. Wang, J. Zhang, P. Liu, H. Sun, X. Zhuang, M. Chen and X. Feng, *Adv. Mater.*, 2018, **30**, 1706279.
22 Y. Zhao, G. Chen, T. Bian, C. Zhou, G. I. Waterhouse, L. Z. Wu, C. H. Tung, L. J. Smith, D. O'Hare and T. Zhang, *Adv. Mater.*, 2015, **27**, 7824–7831.
23 Y. Wang, D. Zhang, W. Peng, L. Liu and M. Li, *Electrochim. Acta*, 2011, **56**, 5754–5758.
24 X. Yan, Q. T. Hu, G. Wang, W. D. Zhang, J. Liu, T. Li and Z. G. Gu, *Int. J. Hydrogen Energy*, 2020, **45**, 19206–19213.
25 W. Yu, N. Deng, K. Cheng, J. Yan, B. Cheng and W. Kang, *J. Energy Chem.*, 2021, **58**, 472–499.
26 J. Hu, X. Tang, Q. Dai, Z. Liu, H. Zhang, A. Zheng, Z. Yuan and X. Li, *Nat. Commun.*, 2021, **12**, 1–10.
27 Z. Xiao, Y. Mei, S. Yuan, H. Mei, B. Xu, Y. Bao, L. Fan, W. Kang, F. Dai and R. Wang, *ACS Nano*, 2019, **13**, 7024–7030.
28 L. Shi, Y. Chen, R. He, X. Chen and H. Song, *Phys. Chem. Chem. Phys.*, 2018, **20**, 16437–16443.
29 J. Luo, Q. Yin, J. Zhang, S. Zhang, L. Zheng and J. Han, *ACS Appl. Energy Mater.*, 2020, **3**, 4559–4568.
30 R. Ramachandran, Y. Lan, Z. X. Xu and F. Wang, *ACS Appl. Energy Mater.*, 2020, **3**, 6633–6643.
31 A. Elgendy, N. El Basiony, F. E. T. Heakal and A. Elkholy, *J. Power Sources*, 2020, **466**, 228294.
32 V. A. Shirin, R. Sankar, A. P. Johnson, H. Gangadharappa and K. Pramod, *J. Controlled Release*, 2020, **343**, 724–754.
33 Z. Cao, B. Li, L. Sun, L. Li, Z. P. Xu and Z. Gu, *Small Methods*, 2020, **4**, 1900343.
34 N. Baig and M. Sajid, *Trends Environ. Anal. Chem.*, 2017, **16**, 1–15.
35 X. Qiao, X. Chen, C. Huang, A. Li, X. Li, Z. Lu and T. Wang, *Angew. Chem., Int. Ed.*, 2019, **58**, 16523–16527.
36 H. Ai, X. Huang, Z. Zhu, J. Liu, Q. Chi, Y. Li, Z. Li and X. Ji, *Biosens. Bioelectron.*, 2008, **24**, 1048–1052.
37 J. Zhou, M. Min, Y. Liu, J. Tang and W. Tang, *Sens. Actuators, B*, 2018, **260**, 408–417.
38 H. Pan, W. Wang, Q. Shen, Y. Pan, L. Song, Y. Hu and Y. Lu, *RSC Adv.*, 2016, **6**, 111950–111958.
39 Y. Cao, D. Zheng, F. Zhang, J. Pan and C. Lin, *J. Mater. Sci. Technol.*, 2022, **102**, 232–263.
40 M. Tabish, G. Yasin, M. J. Anjum, M. U. Malik, J. Zhao, Q. Yang, S. Manzoor, H. Murtaza and W. Q. Khan, *J. Mater. Sci. Technol.*, 2021, **10**, 390–421.
41 X. Xu, S. Shi, Y. Tang, G. Wang, M. Zhou, G. Zhao, X. Zhou, S. Lin and F. Meng, *Adv. Sci.*, 2021, **8**, 2002658.
42 X. Ye, Z. Jiang, L. Li and Z. H. Xie, *Nanomaterials*, 2018, **8**, 411.
43 Y. Tian, C. Dong, G. Wang, X. Cheng and X. Li, *Mater. Lett.*, 2019, **236**, 517–520.
44 M. Zubair, I. Ihsanullah, H. A. Aziz, M. A. Ahmad and M. A. Al-Harthi, *Bioresour. Technol.*, 2020, 124128.
45 X. Zhang, L. Yan, J. Li and H. Yu, *J. Colloid Interface Sci.*, 2020, **562**, 149–158.
46 Y. H. Chuang, Y. M. Tzou, M. K. Wang, C. H. Liu and P. N. Chiang, *Ind. Eng. Chem. Res.*, 2008, **47**, 3813–3819.
47 A. Li, H. Deng, C. Ye and Y. Jiang, *ACS Omega*, 2020, **5**, 15152–15161.
48 W. Xie, Z. Guo, Q. Gao, D. Wang, K. Liang, Z. Gu and L. Y. Zhao, *ACS Appl. Bio Mater.*, 2020, **3**, 5845–5855.
49 L. Yan, M. Zhou, X. Zhang, L. Huang, W. Chen, V. A. Roy, W. Zhang and X. Chen, *ACS Appl. Mater. Interfaces*, 2017, **9**, 34185–34193.
50 X. Liu, A. Zhou, Y. Dou, T. Pan, M. Shao, J. Han and M. Wei, *Nanoscale*, 2015, **7**, 17088–17095.
51 R. Liang, S. Xu, D. Yan, W. Shi, R. Tian, H. Yan, M. Wei, D. G. Evans and X. Duan, *Adv. Funct. Mater.*, 2012, **22**, 4940–4948.
52 C. W. Jeon, S. S. Lee and I. K. Park, *ACS Appl. Mater. Interfaces*, 2019, **11**, 35138–35145.
53 R. Tian, M. Li, H. Teng, H. Luo, D. Yan and M. Wei, *J. Mater. Chem. C*, 2015, **3**, 5167–5174.
54 C. Manzi-Nshuti, P. Songtipya, E. Manias, M. M. Jimenez-Gasco, J. M. Hossenlopp and C. A. Wilkie, *Polymer*, 2009, **50**, 3564–3574.
55 S. Shi, W. Zhang, H. Wu, Y. Li, X. Ren, M. Li, J. Liu, J. Sun, T. Yue and J. Wang, *ACS Sustainable Chem. Eng.*, 2020, **8**, 4966–4974.
56 Y. Xie, Y. H. Gu, J. Meng, X. Yan, Y. Chen, X. J. Guo and W. Z. Lang, *J. Hazard. Mater.*, 2020, **398**, 122862.
57 M. Shao, F. Ning, J. Zhao, M. Wei, D. G. Evans and X. Duan, *Adv. Funct. Mater.*, 2013, **23**, 3513–3518.
58 Z. Li, K. Liu, K. Fan, Y. Yang, M. Shao, M. Wei and X. Duan, *Angew. Chem., Int. Ed.*, 2019, **58**, 3962–3966.
59 G. Mishra, B. Dash and S. Pandey, *Appl. Clay Sci.*, 2018, **153**, 172–186.
60 C. Chen, L. Tao, S. Du, W. Chen, Y. Wang, Y. Zou and S. Wang, *Adv. Funct. Mater.*, 2020, **30**, 1909832.
61 X. Lu, H. Xue, H. Gong, M. Bai, D. Tang, R. Ma and T. Sasaki, *Nano-Micro Lett.*, 2020, **12**, 1–32.
62 X. Li, D. Du, Y. Zhang, W. Xing, Q. Xue and Z. Yan, *J. Mater. Chem. A*, 2017, **5**, 15460–15485.
63 W. Feitknecht and M. Gerber, *Helv. Chim. Acta*, 1942, **25**, 131–137.
64 H. Liang, F. Meng, M. Cabán-Acevedo, L. Li, A. Forticaux, L. Xiu, Z. Wang and S. Jin, *Nano Lett.*, 2015, **15**, 1421–1427.
65 M. Adachi-Pagano, C. Forano and J. P. Besse, *Commun. Chem.*, 2000, 91–92.
66 M. Singh, M. I. Ogden, G. M. Parkinson, C. Buckley and J. Connolly, *J. Mater. Chem.*, 2004, **14**, 871–874.

67 V. V. Naik, T. Ramesh and S. Vasudevan, *J. Phys. Chem. Lett.*, 2011, **2**, 1193–1198.
68 Y. Zhang, L. Wen, X. Bai, N. Song, X. Huang and Y. Li, *Chem. Lett.*, 2019, **48**, 1148–1151.
69 R. Ma, Z. Liu, L. Li, N. Iyi and T. Sasaki, *J. Mater. Chem.*, 2006, **16**, 3809–3813.
70 L. Hui, Y. Xue, B. Huang, H. Yu, C. Zhang, D. Zhang, D. Jia, Y. Zhao, Y. Li and H. Liu, *Nat. Commun.*, 2018, **9**, 5309.
71 K. Cermelj, K. Ruengkajorn, J. C. Buffet and D. O'Hare, *J. Energy Chem.*, 2019, **35**, 88–94.
72 L. Li, R. Ma, Y. Ebina, N. Iyi and T. Sasaki, *Chem. Mater.*, 2005, **17**, 4386–4391.
73 T. Hibino and W. Jones, *J. Mater. Chem.*, 2001, **11**, 1321–1323.
74 T. Hibino, *Chem. Mater.*, 2004, **16**, 5482–5488.
75 J. L. Gunjakar, T. W. Kim, H. N. Kim, I. Y. Kim and S. J. Hwang, *J. Am. Chem. Soc.*, 2011, **133**, 14998–15007.
76 Y. B. Park, J. H. Kim, Y. J. Jang, J. H. Lee, M. H. Lee, B. J. Lee, D. H. Youn and J. S. Lee, *ChemCatChem*, 2019, **11**, 443–448.
77 W. Quan, C. Jiang, S. Wang, Y. Li, Z. Zhang, Z. Tang and F. Favier, *Electrochim. Acta*, 2017, **247**, 1072–1079.
78 J. A. Carrasco, A. Harvey, D. Hanlon, V. Lloret, D. McAteer, R. Sanchis-Gual, A. Hirsch, F. Hauke, G. Abellán and J. N. Coleman, *Commun. Chem.*, 2019, **55**, 3315–3318.
79 M. A. Jobbágy and A. E. Regazzoni, *J. Colloid Interface Sci.*, 2004, **275**, 345–348.
80 C. A. Antonyraj, P. Koilraj and S. Kannan, *Commun. Chem.*, 2010, **46**, 1902–1904.
81 Y. Zhu, Y. Zhou, T. Zhang, M. He, Y. Wang, X. Yang and Y. Yang, *Appl. Surf. Sci.*, 2012, **263**, 132–138.
82 T. S. Munonde, H. Zheng and P. N. Nomngongo, *Ultrason. Sonochem.*, 2019, **59**, 104716.
83 Q. Wu, A. Olafsen, Ø. B. Vistad, J. Roots and P. Norby, *J. Mater. Chem.*, 2005, **15**, 4695–4700.
84 W. Hou, L. Kang, R. Sun and Z. H. Liu, *Colloids Surf., A*, 2008, **312**, 92–98.
85 Y. Wei, F. Li and L. Liu, *RSC Adv.*, 2014, **4**, 18044–18051.
86 J. Li, P. Zhang, X. Zhao, L. Chen, J. Shen, M. Li, B. Ji, L. Song, Y. Wu and D. Liu, *J. Colloid Interface Sci.*, 2019, **549**, 236–245.
87 Y. Wang, Y. Zhang, Z. Liu, C. Xie, S. Feng, D. Liu, M. Shao and S. Wang, *Angew. Chem., Int. Ed.*, 2017, **56**, 5867–5871.
88 Y. Wang, C. Xie, Z. Zhang, D. Liu, R. Chen and S. Wang, *Adv. Funct. Mater.*, 2018, **28**, 1703363.
89 Y. Yan, Q. Liu, J. Wang, J. Wei, Z. Gao, T. Mann, Z. Li, Y. He, M. Zhang and L. Liu, *J. Colloid Interface Sci.*, 2012, **371**, 15–19.
90 H. Li, T. N. Tran, B. J. Lee, C. Zhang, J. D. Park, T. H. Kang and J. S. Yu, *ACS Appl. Mater. Interfaces*, 2017, **9**, 20294–20298.
91 J. Yu, B. R. Martin, A. Clearfield, Z. Luo and L. Sun, *Nanoscale*, 2015, **7**, 9448–9451.
92 J. Yu, J. Liu, A. Clearfield, J. E. Sims, M. T. Speiegle, S. L. Suib and L. Sun, *Inorg. Chem.*, 2016, **55**, 12036–12041.
93 D. Liang, W. Yue, G. Sun, D. Zheng, K. Ooi and X. Yang, *Langmuir*, 2015, **31**, 12464–12471.
94 Y. Zhang, H. Li, N. Du, R. Zhang and W. Hou, *Colloids Surf., A*, 2016, **501**, 49–54.
95 G. Hu, N. Wang, D. O'Hare and J. Davis, *Commun. Chem.*, 2006, 287–289.
96 X. Pang, M. Sun, X. Ma and W. Hou, *J. Solid State Chem.*, 2014, **210**, 111–115.
97 B. M. Hunter, W. Hieringer, J. Winkler, H. Gray and A. Müller, *Energy Environ. Sci.*, 2016, **9**, 1734–1743.
98 B. M. Hunter, J. D. Blakemore, M. Deimund, H. B. Gray, J. R. Winkler and A. M. Müller, *J. Am. Chem. Soc.*, 2014, **136**, 13118–13121.
99 J. Fang, M. Li, Q. Li, W. Zhang, Q. Shou, F. Liu, X. Zhang and J. Cheng, *Electrochim. Acta*, 2012, **85**, 248–255.
100 M. Li, J. Cheng, J. Fang, Y. Yang, F. Liu and X. Zhang, *Electrochim. Acta*, 2014, **134**, 309–318.
101 S. P. Lonkar, J. M. Raquez and P. Dubois, *Nano-Micro Lett.*, 2015, **7**, 332–340.
102 C. Qiao, Y. Zhang, Y. Zhu, C. Cao, X. Bao and J. Xu, *J. Mater. Chem. A*, 2015, **3**, 6878–6883.
103 Q. Q. He, M. J. Zhou and J. M. Hu, *Electrochim. Acta*, 2020, **355**, 136796.
104 E. Scavetta, B. Ballarin, M. Gazzano and D. Tonelli, *Electrochim. Acta*, 2009, **54**, 1027–1033.
105 Y. Wang, Y. Liu, Z. Chen, M. Zhang, B. Liu, Z. Xu and K. Yan, *Green Chemical Engineering*, 2022, **3**, 55–63.
106 Y. Wang, Z. Chen, M. Zhang, Y. Liu, H. Luo and K. Yan, *Green Energy Environ.*, 2021, DOI: **10.1016/j.gee.2021.01.019**.
107 J. Qu, Q. Zhang, X. Li, X. He and S. Song, *Appl. Clay Sci.*, 2016, **119**, 185–192.
108 F. Zhang, N. Du, S. Song, J. Liu and W. Hou, *J. Solid State Chem.*, 2013, **206**, 45–50.
109 T. Iwasaki, K. Shimizu, H. Nakamura and S. Watano, *Mater. Lett.*, 2012, **68**, 406–408.
110 S. Bai, T. Li, H. Wang, L. Tan, Y. Zhao and Y. F. Song, *Chem. Eng. J.*, 2021, **419**, 129390.
111 H. Chi, J. Dong, T. Li, S. Bai, L. Tan, J. Wang, T. Shen, G. Liu, L. Liu and L. Sun, *Green Energy Environ.*, 2020, DOI: **10.1016/j.gee.2020.12.013**.
112 Y. Liu, X. Liang, L. Gu, Y. Zhang, G. D. Li, X. Zou and J. S. Chen, *Nat. Commun.*, 2018, **9**, 1–10.
113 S. Du, Z. Ren, X. Wang, J. Wu, H. Meng and H. Fu, *ACS Nano*, 2022, DOI: **10.1021/acsnano.2c00332**.
114 V. Khusnutdinov and V. Isupov, *Chem. Sustainable Dev.*, 2007, **15**, 367–372.
115 A. N. Ay, B. Zümreoglu-Karan and L. Mafra, *Z. Anorg. Allg. Chem.*, 2009, **635**, 1470–1475.
116 Z. Zhao, X. Zhou, K. Kou and H. Wu, *Carbon*, 2021, **173**, 80–90.
117 W. Wang, H. Yan, U. Anand and U. Mirsaidov, *J. Am. Chem. Soc.*, 2021, **143**, 1854–1862.
118 S. Chen, L. Zhao, W. Wei, Y. Li and L. Mi, *J. Alloys Compd.*, 2020, **831**, 154794.
119 E. H. Mourid, M. Lakraimi and A. Legrouri, *Mater. Chem. Phys.*, 2022, **278**, 125570.

120 X. Bai, J. Liu, Q. Liu, R. Chen, X. Jing, B. Li and J. Wang, *Chem. – Eur. J.*, 2017, **23**, 14839–14847.
121 X. Bai, Q. Liu, Z. Lu, J. Liu, R. Chen, R. Li, D. Song, X. Jing, P. Liu and J. Wang, *ACS Sustainable Chem. Eng.*, 2017, **5**, 9923–9934.
122 X. Su, Y. Wang, J. Zhou, S. Gu, J. Li and S. Zhang, *J. Am. Chem. Soc.*, 2018, **140**, 11286–11292.
123 H. Xu, C. Shan, X. Wu, M. Sun, B. Huang, Y. Tang and C. H. Yan, *Energy Environ. Sci.*, 2020, **13**, 2949–2956.
124 B. Chen, Z. Zhang, S. Kim, S. Lee, J. Lee, W. Kim and K. Yong, *ACS Appl. Mater. Interfaces*, 2018, **10**, 44518–44526.
125 S. Miyata, *Clays Clay Miner.*, 1980, **28**, 50–56.
126 M. Qin, S. Li, Y. Zhao, C. Y. Lao, Z. Zhang, L. Liu, F. Fang, H. Wu, B. Jia and Z. Liu, *Adv. Energy Mater.*, 2019, **9**, 1803060.
127 R. Gao and D. Yan, *Nano Res.*, 2018, **11**, 1883–1894.
128 Q. Xie, Z. Cai, P. Li, D. Zhou, Y. Bi, X. Xiong, E. Hu, Y. Li, Y. Kuang and X. Sun, *Nano Res.*, 2018, **11**, 4524–4534.
129 Y. T. Lai, W. T. Liu, L. J. Chen, M. C. Chang, C. Y. Lee and N. H. Tai, *J. Mater. Chem. A*, 2019, **7**, 3962–3970.
130 P. Bandyopadhyay, X. Li, N. H. Kim and J. H. Lee, *Chem. Eng. J.*, 2018, **353**, 824–838.
131 S. C. Kim, M. S. Islam and S. J. Hwang, *Sol. RRL*, 2018, **2**, 1800092.
132 C. Qiu, X. Hao, L. Tan, X. Wang, W. Cao, J. Liu, Y. Zhao and Y. F. Song, *Chem. Commun.*, 2020, **56**, 5354–5357.
133 X. Jin, T. H. Gu, N. H. Kwon and S. J. Hwang, *Adv. Mater.*, 2021, **33**, 2005922.
134 T. H. Gu, X. Jin, S. J. Park, M. G. Kim and S. J. Hwang, *Adv. Sci.*, 2021, **8**, 2004530.